Design and Preliminary Evaluation of a Dextrous Encounter Type Force Feedback Interface

Anthony Chabrier[1,2], Florian Gosselin[1][a] and Wael Bachta[2][b]

[1]*CEA, LIST, Interactive Robotics Laboratory, F-91120 Palaiseau, France*
[2]*Sorbonne Université, CNRS, UMR 7222 and INSERM, UI 1150,*
Institut des Systèmes Intelligents et de Robotique, F-75005, Paris, France

Keywords: Force Feedback Interface, Encounter Type, Dexterous.

Abstract: Force feedback interfaces aim at allowing natural interactions with a virtual or distant environment with a physical sense of presence. Commercially available systems suffer however two limitations. First, most of them are equipped with a handle whose geometry constraints the movements that can be efficiently simulated to the manipulation of tools shaped like the handgrip. Second, the handle is always grasped in hand and the user feels the friction and inertia of the system even in free space, hence a limited transparency. Dexterous interfaces were introduced to cope with the first issue, while encounter type devices, which are detached from the user's hand and contact it only when haptic feedback is required, allow to tackle the second limitation. To date however, no device efficiently integrates both principles. The aim of this paper is to introduce a new device intended to do so, i.e. to be both dexterous, allowing to simulate any grasp type (limited to two fingers in a first step), and of encounter-type, hence an improved transparency. Its design is presented in details, and first experimental results showing the ability of the device to follow user's movements are introduced.

1 INTRODUCTION

Haptic interfaces allow natural gesture interactions with virtual or remote environments. Therefore, they track the user's movements and provide force feedback generated e.g. when contacts occur between the user's avatar and virtual objects, thus improving the operator's immersion by reproducing a physical sense of presence in the virtual or distant world.

To date, however, commercially available haptic interfaces suffer limitations. Indeed, despite continuous efforts to develop and propose more versatile devices, most of them are still manipulated via a handle fixed at the end of a serial or parallel arm structure (Massie and Salisbury, 1994) (Perret et al., 2013). This simple solution is well suited when simulating an operation performed with a given tool. However, they limit the user's dexterity and are less adapted when manual manipulation is required or when several tools with different shapes are used successively. In this case, a dexterous interface is required.

Designing a dexterous haptic interface is however an extremely difficult task due to the complexity of the hand kinematics, inter-individual variability, and great sensitivity of the human hand (see for example recent reviews of dexterous haptic interfaces in (Heo et al., 2012) and (Perret and Vander Poorten, 2018)). To tackle this issue, researchers often propose a simplified design allowing the measurement of all hand's movements but providing force feedback in only some directions, usually opposite to the fingers' flexion. Despite lighter and more compact, such designs can only resist hand closure and do not allow simulating the forces occurring when touching the virtual objects in any arbitrary direction. Therefore, miniature robots with several degrees of freedom (DoFs) allowing multi-directional force feedback are needed for each finger. This solution theoretically allows the rendering of any force on the fingers. However, their structure is in turn complex, cumbersome and heavy. Also, their transparency is often limited, as small motors with multistage reducers are required to keep volume and weight

reasonable. This affects the user's ability to make abstraction of the interface and prevents natural gestures. Preserving a high transparency and in particular a high haptic sensitivity is however of particular importance for fine manipulation, i.e. when grasping and precisely manipulating small objects.

To overcome this limitation, researchers proposed to implement intermittent contacts (Mc Neely, 1993) (Yoshikawa and Nagura 1997), i.e. the user is no more in contact with the device in free space. The device remotely follows his movements and comes into contact with the hand only when he touches a virtual object. This way, a perfect transparency is achieved in free space. Furthermore, the transition between free space and contact is also more natural as it is rendered via a physical contact with the robot in the real world. This greater sensitivity is particularly interesting during fine manipulation tasks.

It is worth noting however that, to date, none of the two alternative solutions existing for the implementation of the intermittent contact paradigm, i.e. encounter and encountered-type interfaces, allows simulating dexterous interactions in a perfect way:

- On the one hand, the underlying principle of encountered-type haptic interfaces is to use a robot whose end effector moves on the surface of the closest to the user virtual object and waits for him to come into contact with it, the robot being often static in this phase. This end effector has usually a shape similar to the simulated objects, or it is composed of several basic geometric primitives (e.g. planes, corners, edges,…). As a result, it can only simulate objects having this given shape, which was initially most of the time fixed (Tachi et al., 1994) (Yokokohji et al., 1995), even if some more recent devices propose reconfigurable end-effectors (Yokokohji et al., 2005) (De Araujo et al., 2010). Even so, the simulation is limited to given classes of objects and the device cannot really be called dexterous.

- On the other hand, encounter-type devices usually carry a hollow shaped end-effector that surrounds the user's finger and closely tracks it without colliding with it in free space. When the user moves towards the environment, the interface slows down so that the end-effector enters in contact with the finger at the exact position and time the avatar collides with the virtual environment. Such devices theoretically allow a greater freedom than encountered-type interfaces in terms of the variety of objects that can be simulated. However, most of them allow interacting with only one finger (Hirota and Hirose, 1993) (Yoshikawa and Nagura 1997,

1999) (Gonzalez et al., 2015a). Only few encounter-type interfaces with several fingers exist (Nakagawara et al., 2005) (Fang at al., 2009), but they are not as transparent in free space as mono-finger's ones as they make use of optical IR tracking systems with reflective plates resting on fingers to measure their movements. Also, they are unfortunately not really dexterous. Indeed, their joints are coupled, thus limiting the fingers' movements to some given synergies. Moreover, force feedback is limited to flexion-extension. They can thus simulate the resistance of an object grasped in hand, but they do not allow simulating forces occurring in any arbitrary direction (e.g. external forces exerted on this object, or friction associated with tangential movements along a surface).

In this paper, we present the design and preliminary evaluation of a device that is intended to tackle the above-mentioned limitations. It is:

- More dexterous than existing intermittent contact devices, i.e. it can track and apply forces on several fingertips in any direction, allowing to simulate different grasp types.
- More transparent than existing dexterous interfaces thanks to its truly intermittent-contact nature, i.e. it is not at all in contact with the fingertips in free space.

The main innovation of this device is the combination of intermittent contacts and dexterity, each capacity being derived from the best practices. Regarding intermittent contacts, it relies on the encounter type paradigm which was shown above to be the most promising solution for the implementation of a dexterous haptic interface. Regarding dexterity, it is based on the use of small 6 DoF robots with 3 DoF force feedback on each finger (limited to two fingers in a first step).

2 DESIGN AND IMPLEMENTATION

2.1 Specifications

The following criteria were considered for the specification of our interface:

1/ Fine dexterous manipulation: our aim is to develop a device allowing the simulation of fine dexterous manipulation. Therefore several grasp types are required to adapt to the manipulated tools and objects (Feix et al., 2009). This calls for a dexterous device allowing natural interactions with

the palm and fingers. Also, the links and joints have to be positioned and dimensioned so that the robot does not limit the fingers' movements.

2/ Universal fit: two types of dexterous interfaces can be found in the literature. Exoskeletons have links and joints similar to the hand, and they are attached to every phalanges on which they can independently apply forces. They allow simulating both precision and power grasps, at the price however of strong mechanical constraints as their joints have to be roughly aligned with the fingers' ones. Hence, they must be tuned to each user, which is not convenient for a universal device that can be used by different operators. On the contrary, fingertip interfaces are fixed only on the palm and distal phalanges. Despite being restricted to the simulation of precision grasps, they can more easily fit different users and their design is much simpler. Our application being mainly focused on precise manipulation, we decided to develop a fingertip haptic interface for the thumb and index fingertips as in (Gosselin et al., 2005) and (Frisoli et al. 2007). This is sufficient for the manipulation of small objects.

3/ High transparency and force feedback quality: haptic interfaces should be transparent in free space, i.e. display a mechanical impedance that is sufficiently low for the user to forget their presence. They should also be able to provide high impedances to simulate realistic contacts with stiff surfaces. This contradiction usually leads to a compromise between a high transparency in free space (i.e. low friction and inertia) and realistic force feedback in contact (i.e. high forces and stiffness). To overcome this limitation, we will implement intermittent contacts. It is worth noting that a single finger can apply almost only forces on objects, torques being generated by a combined use of several fingers. Consequently, only 3D force feedback is required at the fingertips.

4/ Fatigueless use: glove-type interfaces, even optimized, often remain relatively heavy and lifting the device is quickly tiring if it is worn on the hand or arm. To cope with this problem, we will mount the device on a passive counterbalancing system.

2.2 Electro-Mechanical Design

2.2.1 Overview of the System

The two fingers encounter-type dexterous haptic interface developed to answer the above-mentioned specifications is illustrated in Figure 1. It is composed of two robots equipped with intermittent contact hollow-shaped end-effectors facing the thumb and index fingertips and a basis grasped with the

remaining fingers (this is an interim solution until the development of an encounter type palm tracking system). The whole interface is mounted on a passive counterbalancing system and it is linked with an external controller. Each of these components will be presented in details below.
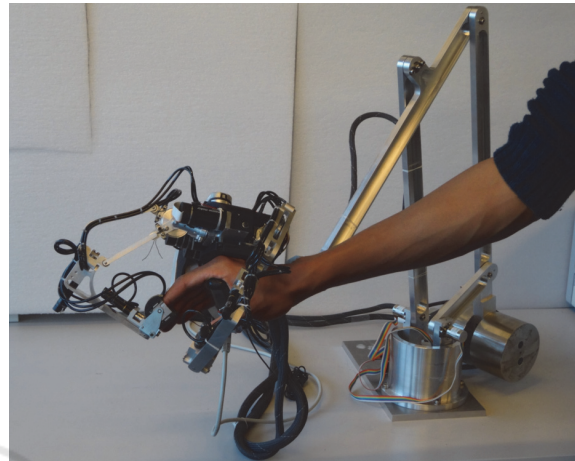

Figure 1: Encounter-type dexterous haptic interface prototype.

2.2.2 Fingers' Robots

The index finger has four DoF, the thumb five. One could think that robots with the same movement capabilities are sufficient to follow the movements of these fingers. This requires however that at least some of the robots' joints are aligned with the fingers' ones. This cannot be guaranteed here as the glove will be used by different users having various hand sizes and morphologies. It is also worth noting that we intend to use an encounter type solution for the palm in the future. In this case, the device will no more be fixed on the hand and the position of the robots relative to the palm will vary during operation. In these conditions, the robots must have 6 DoF to be able to follow any fingers' movements.

In practice, such 6 DoF structures are usually obtained with separate positioning and orientation stages allowing to displace the end-effector, resp. to orient it. This efficient solution, illustrated in Figure 2 for the index finger, will be used here.

As already mentioned in section 2.1, it is worth noting that a single finger can apply almost only forces on the environment, torques being generated by a combined use of several fingers. Only 3D force feedback is thus required at the fingertips. Still, the robots should accommodate the distal phalanx' changes in orientation occurring during hand closure.
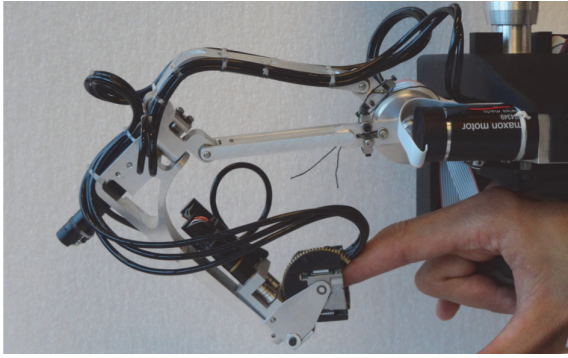
Figure 2: Index finger's robot architecture.

In classical force feedback gloves, the rotation joints are passive. However, due to the intermittent nature of our device, the robot's end effector will be detached from the fingertip in free space. As a consequence, it will not follow the fingertip passively and the end effector has to be actively oriented.

2.2.3 Kinematics

The positioning stage of our device is composed of a pivot joint and a parallelogram as in (Massie and Salisbury, 1994), and the actuators are fixed on the palm in order to reduce the robot's moving parts inertia, their movements being transmitted to the joints using cables. The pivot joint is tilted and shifted upwards as proposed in (Gosselin at al., 2005) to ensure that the fingertip will never cross this axis, which would lead to a singular configuration.

The links' dimensions were optimized in CAD so that the devices' workspace encompasses the range of motion of the fingers, expanded to take into account the encounter-type related clearance between the fingers and the end-effector (plus a clearance between the palm and the basis as the later will also be of encounter-type in the future). We made here the assumption that the total clearance will remain below 15mm (3mm for the fingertips plus 12mm for the palm, these values being computed taking into account the user's and robot dynamics using the methodology proposed in (Gonzalez et al., 2015b)). With these assumptions, we iteratively dimensioned the links, with additional constraints on the absence of collisions with the fingers and on the integration of the end-effector and orientation stage actuators. Optimal dimensions are: 10° tilt angle relative to the horizontal for the index (0° for the thumb), length of the first, second and third links respectively equal to 40mm, 95mm and 86mm. With these dimensions, the robots can span the index finger and thumb's workspaces inflated by 15mm (see Figure 3 for the index, similar results were obtained for the thumb).
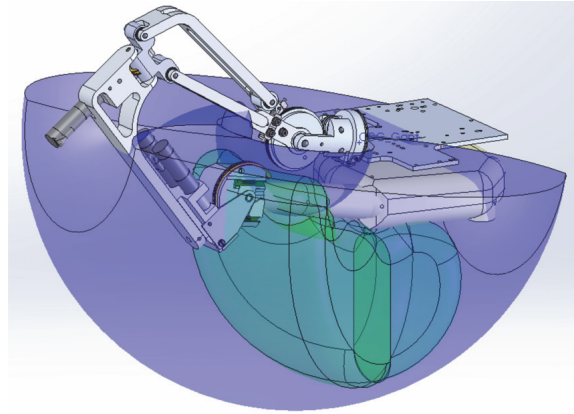

Figure 3: Inflated index finger's (in green) and robot's (in blue) workspace.

The orientation stage is composed of three pivot joints with intersecting axes, whose range of motion were iteratively adjusted so as to accommodate the index and thumb reorientations occurring during hand's movements.
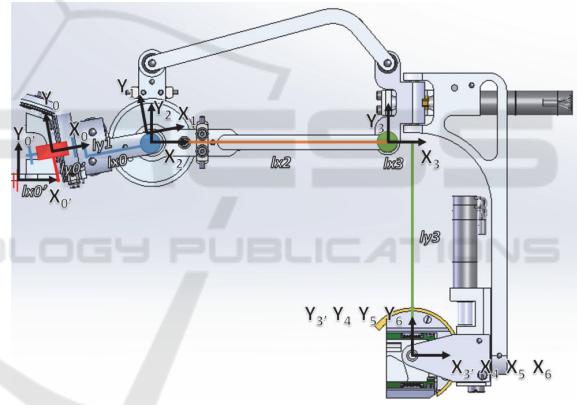

Figure 4: Index finger's kinematics.

With the notations given in Figure 4, the geometric model of the robot can be written as:

$$T_{0'0}=trans(X_{0'},l_{x0'}).trans(Y_{0'},l_{y0'}).rot(Z_{0'},q_{z0'}) \quad (1)$$

$$T_{01}=trans(X_0,l_{x0}).\ rot(X_1,q_1) \quad (2)$$

$$T_{12}=trans(Y_1,-l_{y1}).rot(Z_2,q_2-q_{z0'}) \quad (3)$$

$$T_{23}=trans(X_2,l_{x2}).rot(Z_3,q_3) \quad (4)$$

$$T_{33'}=trans(X_3,l_{x3}).trans(Y_3,-l_{y3}) \quad (5)$$

$$T_{3'4}=rot(Y_{3'},q_4).rot(Z_4,q_{z4}) \quad (6)$$

$$T_{45}=rot(X_4,q_5) \quad (7)$$

$$T_{56}=\ rot(Z_5,q_6) \quad (8)$$

With q_{z4} an additional parameter introduced for the thumb's robot whose forearm is slightly tilted

compared to the index' one in order to avoid collisions with the thumb (q_{z4}=0 for the index).

2.2.4 Actuation

To select the actuators of the positioning stage (which acts as an encounter type haptic interface), both free space and contact modes must be considered:

- In contact mode, the robot should be able to sustain the fingers' forces, typically in the range between 5N continuous and 15N during few seconds (Gonzalez et al., 2014). To compute the associated motor torques, we use force dimensioning ellipsoids as explained in (Gosselin, 2016). Another constraint in contact mode is to have a robot that is sufficiently stiff to allow for the simulation of hard surfaces. Theoretically, a stiffness above 24N/mm is required to simulate a rigid surface without visual feedback (Tan at al., 1994). It is however possible to rely on the vision predominance over haptics to give the illusion of stiffness with a much lower rigidity when vision is available. Here, we set our requirement at 10N/mm.
- Regarding free space, the robot should have a sufficient acceleration capacity to follow the user's movements without colliding with his or her fingers.

The actuators selected after an iterative optimization taking into account the above-mentioned criteria but also transparency and integration constraints are Maxon DC motors (ref. RE25 339152, 20W, 24V, 115g, max. torque 30.4mN.m continuous, 325mN.m peak) equipped with 256ppt encoders, associated with a cable capstan reducer to keep the system highly backdriveable. In order to limit the size of the reduction stage, we used two stages reducers and made use of miniature Dyneema cables which can bend narrower than steel cables (ref. Berkley Whiplash 1077221, 0.28mm, 44.9kg resistance). The first stage has a reduction ratio of 4:1 and the second stage a ratio of 6:1 on the abduction-adduction axis (hence an output torque of 730mN.m) and 7:1 on the other axes (output torque 851mN.m).

Regarding orientations, there is no need for backdriveability. The only requirement is it follow the fingers' change in orientation at a sufficient speed. Here, to allow for a simple and compact design, we used small and light actuators which are integrated directly in the orientation stage, and worm and wheel gears to both actuate the end-effector and sustain the force applied by the user once in contact. Such systems are highly compact, yet they are not backdriveable and naturally resist external forces. After a careful review

of the components available, we selected miniature Maxon DC motors (réf. RE10 256105, 1.5W, 12V, 10g, max. torque 1.55mN.m continuous, 3.24mN.m peak) equipped with 10ppt encoders. They are associated with 16:1 planetary gearheads (ref. GP10A 218416) and HO58 worm and 25 teeth HO59/7 wheels on the two first axes and with a 4:1 planetary gearhead (ref. GP10A 218415) and a HO58 worm and a 75 teeth HO59/11 wheel on the last axis.

2.2.5 Hollow Shaped End-effector

In an encounter type device, the end effector serves as a contact surface only when force feedback is required. In free space, it must follow the finger remotely without entering in contact with it. Therefore, a sufficient clearance must be provided to allow the robot accelerating and catching up the finger when the later moves. This clearance depends on the fingertip and robot's dynamics. To design the end-effector, we used the same hypotheses as in (Gonzalez et al., 2015b), i.e. maximum finger speed and acceleration of 1.26m/s and 24.5m/s² in flexion-extension and 0.26m/s and 4m/s² in abduction-adduction and robot dynamics similar to those of the first axis of the PHANToM Premium 1.5 High Force. In these conditions, the tracking errors remain below 3.1mm in flexion-extension and 0.6mm in abduction-adduction. Taking the fingers dimensions into account, we arrive at a cylinder with a diameter of 24mm for the index and 28mm for the thumb. The configuration of the finger inside the end-effector is measured with nine infrared proximity sensors (ref. Vishay VCNL4010). As shown in Figure 5, eight of them are placed around the distal phalanx in two different planes, the last one being in front of the fingertip. It is worth noting that no sensor is placed in front of the finger pulp, allowing to minimize the thickness of the end-effector below the finger.
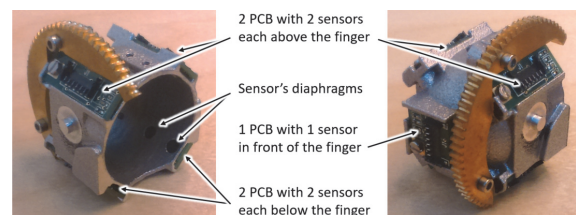

Figure 5: Placement of the proximity sensors in the end-effector.

The ability of this end-effector to measure the position and orientation of the finger was carefully checked. It is capable of measuring the movements of a fingertip in the ranges of 1-10mm in all directions, ±10° in abduction/adduction and ±20° in flexion/

extension, with errors about 0.2mm and 0.4° near the center of the end-effector (Chabrier et al., 2017).

2.2.6 Fixed Basis

For an optimal transparency of the system, intermittent contacts should also be implemented on the palm, so that the robot doesn't touch the hand at all in free space. In a first step however, for the sake of simplicity, we decided to equip the basis on which the index and thumb robots are fixed with a handle grasped with the remaining fingers. Their position and orientation on the basis are optimized in CAD so that they can follow the fingers' movements over their workspace.

2.2.7 Counterbalancing System

A passive counterbalancing system is used to compensate for the weight of the device which is too heavy to be worn on the hand. In practice, we advantageously make use of a pantograph architecture (ratio 3:1) equipped with a counterweight (mass 7.43kg, see Figure 1). This solution allows to keep the distance ratio between the interface's centre of mass, the axes of the pantograph and the counterweight unchanged. This way, the weight of the glove is compensated in any position in the workspace of the supporting arm. This system is further equipped with 15-bits angular encoders (ref. Gurley A19), allowing for the measurement of the hand position in space with a minimum resolution of 0.14mm. A passive orientation system is added to allow for the glove to move freely in orientation. Its axes intersect at the centre of mass of the glove (fingers extended) so that no torque is generated on the hand. 12 bits angular encoders are used on these axes (ref. CUI AMT11), hence a resolution of 0.09° on the hand orientation.

2.2.8 Electronics

Our interface integrates 18 encoders (6 on each robot of the glove plus 6 in the supporting arm), 18 infrared sensors (9 in each end-effector) and 12 actuators. The electronics monitoring the data from all these sensors and controlling the motors should work at a frequency that is sufficient for a stable and performant control of the device, typically in the order of 1 kHz. To reach this requirement, we use components linked with an EtherCAT bus. For the measurement of the fingertip's position in the end-effector, a custom designed card based on a FPGA was developed. It allows measuring the 18 signals of the proximity sensors in parallel at a framerate higher than 1kHz. For the measurement of the supporting arm's encoders, we use Beckhoff EL5002 units connected to the Gurley A19 sensors via a SSI bus and Beckhoff EL5101 units connected to the CUI AMT11 encoders. Finally, the motors and motors' encoders are connected to 2 Technosoft 6 axes iPOS360x SY-CAT cards each equipped with 3 iPOS3602 VX-CAN and 3 iPOS3604 VX-CAN servo-drives (the former can deliver a maximum current of 3.5A that fits the RE25, the later a maximum current of 1A well adapted for the RE10). This solution allows all data to be properly synchronized and transmitted to a master controller by the same fieldbus.

3 CONTROLLER

3.1 Introduction

As shown in Figure 6, encounter type haptic interfaces can be in three different states: 1- free space, where the main goal is to follow the finger's movements at a close distance without entering in contact with it, 2- contact, where force feedback should be generated in a proper and stable way, and 3- transition, which should properly manage the transition between previous modes so that the finger encounters the end effector of the robot at the exact place of the obstacle and the exact avatar contact time.
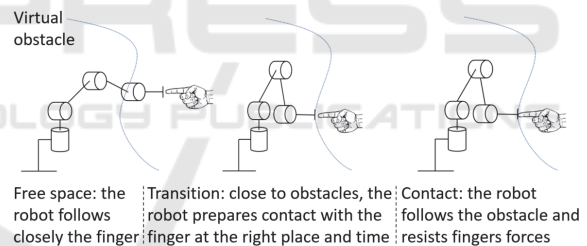

Figure 6: Encounter type interface principle of operation.

Impedance control is usually used to control such devices, both in free space and contact modes. However, the reference position is different in both conditions, the goal being to keep the fingertip center at the centre of the hollow end-effector in free space while the fingertip pulp is in contact with the end-effector's inner surface in contact modes. (Gonzalez et al., 2015a) has shown that abrupt transitions between these modes produce instabilities and that smooth transitions are preferable as they remain stable (provided carefully adjusted gains).

The situation is slightly different here, as we have to manage both the positioning stage which functions as an encounter type device, and the orientation stage, which is more simply controlled in speed in order to follow the fingertip orientation. Details on the controller are given below.

3.2 Positioning Stage

3.2.1 Control in Free Space

In free space, the end effector should remotely follow the fingertip without any collision. We use therefore an impedance control scheme intended to minimize the Cartesian error $\varepsilon_{f/e,X}$ between the absolute position $X_{e/0}$ of the centre of the end-effector and the absolute position $X_{f/0}$ of the fingertip. In practice, this control scheme is implemented at the joint level to increase the robustness of the controller (Plumet et al., 1995), the tracking torque τ_t being function of the position error $\varepsilon_{f/e,q}$ computed in the joint space using the robot's Jacobian Matrix $J(q)$. A proportional and derivative controller with properly tuned gains is used for stability reasons (see Figure 7).
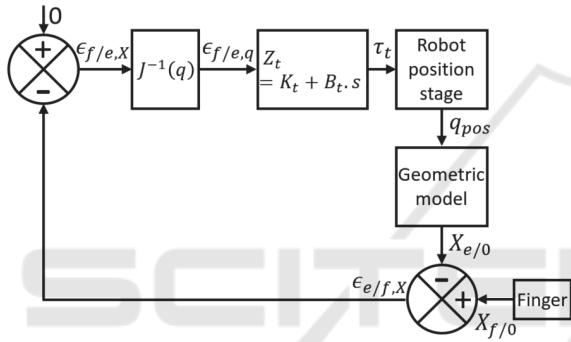
Figure 7: Positioning stage control in free space.

3.2.2 Contact Mode

In contact mode, the fingertip is in contact with the end-effector's inner surface which is in charge of force rendering. The user's skin being then at the same position as the end effector's inner surface, the penetration $\varepsilon_{f/vo,X}$ of the fingertip in the virtual obstacle (vo), that is the distance between the skin (obtained as $X_{f/0} - R_f$ with $X_{f/0}$ the position of the fingertip's centre and R_f the fingertip radius) and the obstacle $X_{vo/0}$, is equal to the distance between the end-effector's inner surface (obtained as $X_{e/0} - R_e$ with $X_{e/0}$ the position of the end effector and R_e its radius) and the obstacle. Hence we have $\varepsilon_{f/vo,X} = X_{f/0} - R_f - X_{vo/0} = \varepsilon_{e/vo,X} = X_{e/0} - R_e - X_{vo/0}$.
The resulting interaction forces are calculated using a modified Kelvin-Voigt model (Achhammer et al., 2010) with the hypothesis that virtual obstacles are modelled as viscoelastic elements without tangential friction. With $\dot{\varepsilon}_{f/vo,X}$ the derivative of $\varepsilon_{f/vo,X}$, the controller can be expressed as $Z_{vo} = K_{vo} + B_{vo}.s$ if $\dot{\varepsilon}_{f/vo,X}$ is negative, $Z_{vo} = K_{vo}$ if $\dot{\varepsilon}_{f/vo,X}$ is positive.
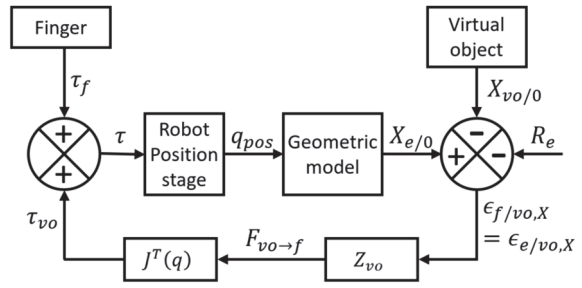

Figure 8: Positioning stage control in contact mode.

3.2.3 Transitions

Transitions have to be initiated as soon as the user's avatar is close enough to the virtual obstacles. Here, we propose to take advantage of the fact that, in free space, the inner surface of the end defector is always in advance to the finger and will thus approach the obstacles before the finger. In practice, we propose to initiate the transition as soon as the end-effector's inner surface encounters the obstacle. The main goal is then to ensure that the end-effector's inner surface remains positioned at the surface of the virtual obstacle and to stabilize it before the finger contacts it. As shown on Figure 9, this principle can be implemented in a similar way as the contact mode. However the goal is here to stabilize the ring as quickly as possible, i.e. with the highest possible yet stable gains K_s and B_s, while the gains in contact mode are expected to simulate the objects behaviour and can be lower.
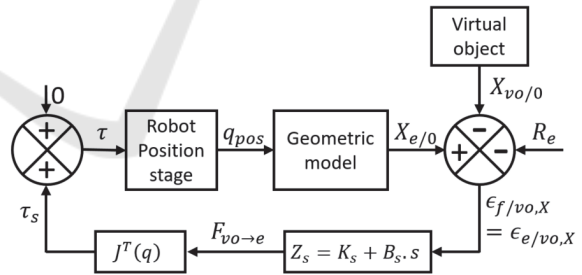

Figure 9: Positioning stage control during stabilisation.

It should be noticed that, in practice, such proposal still introduces a transition between the free space and stabilization phases. In order to avoid instabilities at that moment, we implement a smooth transition that proves to be stable if the gains are chosen adequately (Gonzalez et al., 2015a). Therefore we introduce a function $\beta(t)$ that varies linearly between 0 and 1 and implement a combination of the tracking torque τ_t and stabilisation torque τ_s for a short time just before the transition mode (i.e. $\tau = \beta(t).\tau_t + (1 - \beta(t)).\tau_s$).

A transition also occurs between the stabilization phase and the contact mode. As the control scheme is the same, except different gains, we simply manage this transition through gains scaling, which are initiated as soon as the end-effector' speed is low enough, meaning that it is already stabilized.

The global control scheme combining free space, free space to stabilization transition, stabilization phase, transition to contact and contact state is illustrated in Figure 10.
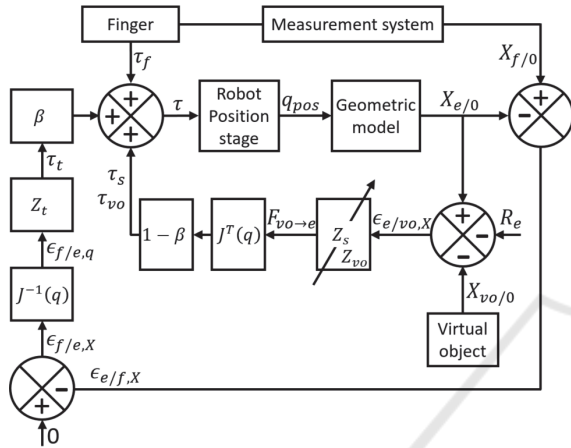

Figure 10: Global control scheme in position.

3.3 Orientation Stage

For the orientation stage, we use a simple joint speed control based on the sampling time t_{samp} (speed control is preferred over impedance control in this case as the orientation stage's encoders have a very low resolution which limits the gains that can be implemented in an impedance controller to unusable values).
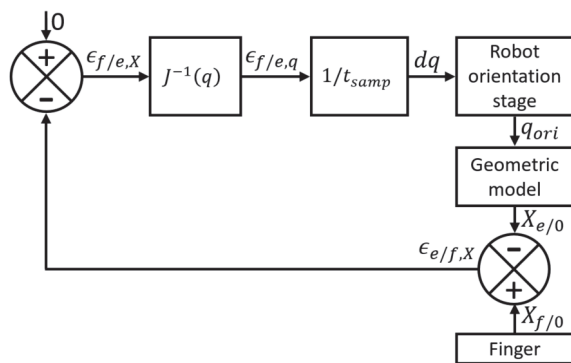

Figure 11: Orientation stage control.

It is worth noting that while several control modes are required for the positioning stage, the controller always remains the same for the orientation stage.

4 PRELIMINARY EVALUATION

The haptic interface presented in this paper as well as its controller are still under development and we were only able to test the index finger's robot's behaviour, and only in free space and contact modes.

4.1 Free Space Finger Tracking

The first tests were intended to verify the ability of the system to follow the index finger in free space. The positioning stage being similar to previous systems developed by the authors which have already been demonstrated functioning well (Gonzalez et al., 2015a), (De La Cruz Fierro et al., 2017), we focused more specifically on the orientation stage. The positioning stage was blocked in position and the orientation stage was controlled in speed to follow the finger's movements. Figure 12 illustrates the movements used during these tests. They correspond to a range of motion of about 30° in abduction-adduction and about 70° in flexion-extension (as the position of the end-effector is fixed, the user has to move his hand to rotate the end-effector). Figures 13 and 14 illustrate the results obtained (the amplitude of the movement is measured by the orientation stage and the error is measured by the end effector).
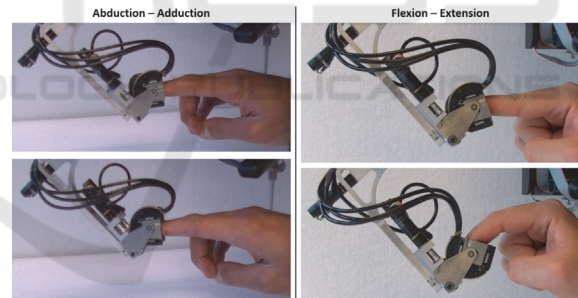

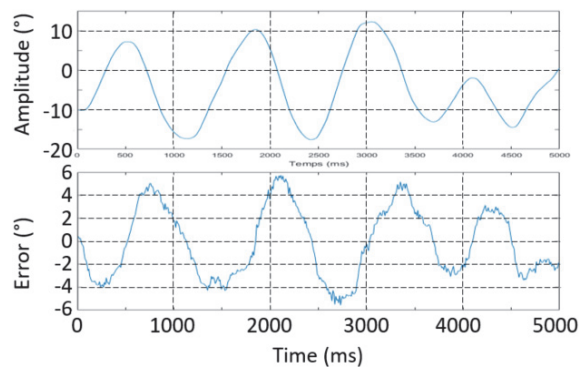Figure 12: Hand movements used for finger's tracking tests.

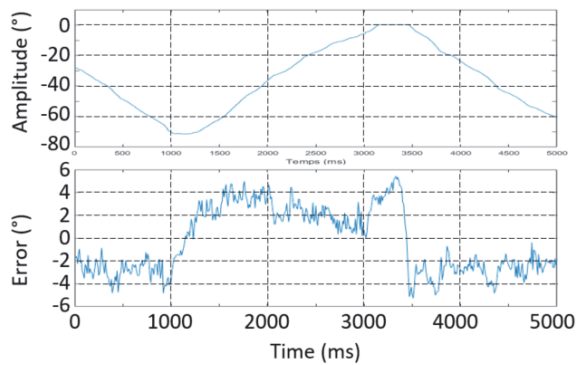Figure 13: Tracking movement amplitude and tracking error in abduction-adduction.

Figure 14: Tracking movement amplitude and tracking error in flexion-extension.

The error remains below 6° for both movements (for movements combining abduction and flexion, it remains below 10°). This is sufficient in practice to avoid finger end-effector contacts in free space.

4.2 Force Feedback at Contact

We also tested the ability of the device to render forces in contact. Therefore, we performed movements in abduction-adduction and flexion-extension of relatively small amplitude to minimize the influence of the orientation stage (see Figure 15). The object's stiffness is arbitrarily set at 1500N/m.
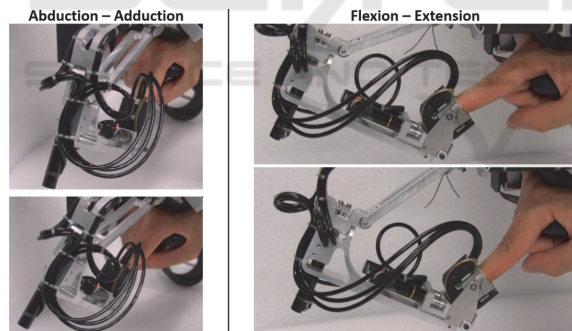

Figure 15: Hand movements for the force feedback tests.
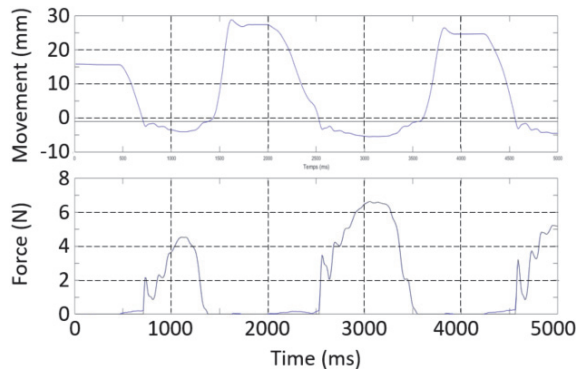

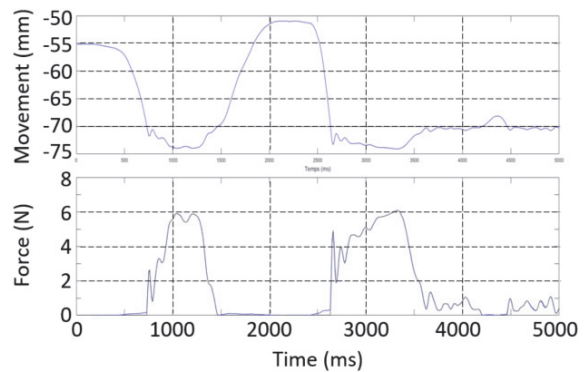Figure 16: Force tests results in abduction-adduction.

Figure 17: Force tests results in flexion-extension.

Figures 16 and 17 illustrate the results obtained. We can see that the force is effectively null in free space and appears only when touching the environment as expected.

5 CONCLUSIONS AND PERSPECTIVES

This paper presents the design and preliminary evaluation of a novel haptic interface that is both dexterous and of encounter type. First results show that this device performs well both in tracking the fingertip of the index in orientation and in applying force on it, thus validating the proposed design. Future work will concern both the management of the transition between both modes and the control of the thumb's robot. In a longer term, we plan to couple this interface with a VR application allowing to test its ability to perform dexterous tasks in VR with a high degree of realism. A particular attention should be given to the simulation of the friction between the fingers and the grasped object, using e.g. an advanced Coulomb-Contensu model as in (Gosselin et al., 2020), in order to be able to render a tight or a loosen grip in a natural way. On a longer term, the passive counterbalancing system should be replaced with an active carrying robot in order to allow rendering torques on the palm. Finally, we also intend to work on the development of an encounter type palm tracking system.

ACKNOWLEDGEMENTS

services), and partly accomplished within the laboratory of excellence SMART supported by French state funds managed by the ANR within the Investissements d'Avenir program (ANR-11-IDEX-0004-02).

REFERENCES

Achhammer, A., Weber, C., Peer, A., Buss, M., (2010), Improvement of model-mediated teleoperation using a new hybrid environment estimation technique, *Proc. IEEE Int. Conf. on Rob. and Autom.,* pp. 5358–5363.

Chabrier, A., Gosselin, F., Gonzalez, F., Bachta, W., (2017), Design and experimental evaluation of an infrared instrumentation for haptic interfaces, *Proc. IEEE Int. Instrumentation and Measurement Technology Conf.*, pp. 724-729.

De Araujo, B.R., Guerreiro, T., Fonseca, M.J., Jorge, J.A., Pereira, J.M., Bordegoni, M., Ferrise, F., Covarrubias, M., Antolini, M., (2010), An haptic-based immersive environment for shape analysis and modelling, *Journal of Real-time Image Processing*, 5, pp. 73–90.

De La Cruz Fierro, O., Bachta, W., Gosselin, F., Morrel, G., (2017), A New Control Strategy for the Improvement of Contact Rendering with Encounter-Type Haptic Displays, *Proc. Int. Conf. on Informatics in Control, Automation and Robotics*, pp 471-480.

Fang, H., Xie, Z., Liu, H., (2009), An exoskeleton master hand for controlling DLR/HIT hand, *Proc. of the IEEE Int. Conf. on Intel. Robots and Systems*, pp. 3703–3708.

Feix, T., Pawlik, R., Schmiedmayer, H.B., Romero, J., Kragic, D., (2009), A Comprehensive Grasp Taxonomy, *Robotics, Science and Systems Conference: Workshop on Understanding the Human Hand for Advancing Robotic Manipulation.*

Frisoli, A., Simoncini, F., Bergamasco, M., Salsedo, F., (2007), Kinematic design of a two contact points haptic interface for the thumb and index fingers of the hand, *ASME Journal of Mechanical Design*, 129.5, pp. 520–529.

Gonzalez, F., Gosselin, F., Bachta, W., (2014), Analysis of hand contact areas and interaction capabilities during manipulation and exploration, *IEEE Trans. on Haptics*, 7(4), pp. 415-429.

Gonzalez, F., Bachta, W., Gosselin, F., (2015a), Smooth transition-based control of encounter-type haptic devices, *Proc. IEEE Int. Conf. on Robotics and Automation*, 2015, pp. 291-297.

Gonzalez, F., Gosselin, F., Bachta, W., (2015b), A 2D infrared instrumentation for close-range finger position sensing, *IEEE Trans. on Instrumentation and Measurement*, 64(10), pp. 2708-2719.

Gosselin, F., (2016), Modern devices for telesurgery, *The e-medecine, e-health, m-health, telemedicine and telehealth handbook*, CRC Press, Taylor and Francis, Vol. 2, Section 1, pp. 37-59.

Gosselin, F., Andriot, C., Keith, F., Louveau, F., Briantais, G., Chambaud, P., (2020), Design and integration of a dexterous interface with hybrid haptic feedback, *Proc. Int. Conf. on Informatics in Control, Automation and Robotics*, 9 pages.

Gosselin, F., Jouan, T., Brisset, J., Andriot, C., (2005), Design of a wearable haptic interface for precise finger interactions in large virtual environments, *Proc. IEEE Worldhaptics Conf.*, pp. 202–207.

Heo, P., Min Gu, G., Lee, S.J., Rhee, K., Kim, J., (2012), Current Hand Exoskeleton Technologies for Rehabilitation and Assistive Engineering, *Int. J. Precision Engineering and Manufacturing*, 13(5), pp. 807-824.

Hirota, K., Hirose, M., (1993), Development of surface display, *Proc. IEEE Virtual Reality Annual International Symposium*, pp. 256–262.

Massie, T., Salisbury, J.K., (1994), The PHANTOM haptic interface: A device for probing virtual objects, *Proc. ASME Symp. on Haptic Interfaces for Virtual Environment and Teleoperator Systems*, pp. 295–299.

McNeely, W., (1993), Robotic graphics: a new approach to force feedback for virtual reality, *Proc. IEEE Int. Symp. on Virtual Reality*, pp. 336 –341.

Nakagawara, S., Kajimoto, H., Kawakami, N., Tachi, S., Kawabuchi, I., (2005), An encounter-type multi-fingered master hand using circuitous joints, *Proc. IEEE Int. Conf. on Rob. and Autom.*, pp. 2667–2672.

Perret, J., Kneschke, C., Vance, J., Dumont, G., (2013), Interactive Assembly Simulation with Haptic Feedback, A*ssembly Automation*, 33 (3), pp. 214-220.

Perret, J., Vander Poorten, E., (2018), Touching Virtual Reality: A Review of Haptic Gloves, *Proc. Int. Conf. on New Actuators,* pp. 270-274.

Plumet, F., Morel, G., Bidaud, P., (1995), Shall we use a dynamic model to control the motions of industrial manipulators?, *Proc. 9th World Congress on the Theory of Machines and Mechanisms*, pp. 235–240.

Tachi, S., Maeda, T., Hirata, R., Hoshino, H., (1994), A construction method of virtual haptic space, *Proc. Int. Conf. on Art. Real. and Tele-Existence*, pp. 131–138.

Tan, H.Z., Srinivasan, M.A., Eberman, B., Cheng, B., (1994), Human factors for the design of force-reflecting haptic interfaces, *Dynamic Systems and Control*, 55.1, pp. 353-359.

Yokokohji, Y., Hollis, R.L., Kanade, T., (1996), What you can see is what you can feel – development of a visual/haptic interface to virtual environment, *Proc. IEEE Virtual Reality Annual Int. Symp.*, pp. 46–53.

Yokokohji, Y., Muramori, N., Sato, Y., Yoshikawa, T., (2005), Designing an encountered-type haptic display for multiple fingertip contacts based on the observation of human grasping behaviors, *International Journal of Robotics Research*, 24(9), pp. 717–729.

Yoshikawa, T., Nagura, A., (1997), A touch and force display system for haptic interface, *Proc. IEEE Int. Conf. Rob. Autom.*, pp. 3018–3024.

Yoshikawa, T., Nagura, A., (1999), A three-dimensional touch/force display system for haptic interface, *Proc. IEEE Int. Conf. on Robot. and Autom.*, pp. 2943-2951.